TEMPLATE DIRECTED FORMATION OF METALLIC In / (0001) SURFACE OF Sb₂Te₃ 2D LAYERED SEMICONDUCTOR SELF-ASSEMBLING NANOSYSTEM

P.V. Galiy[1], T.M. Nenchuk[1], A. Ciszewski[2], P. Mazur[2], O.V. Tsvetkova[1], V.I. Dzyuba[1], T.R. Makar[1]

[1]Ivan Franko Lviv National University,
50 Dragomanov Street, Lviv, 79005, Ukraine

[2]Institute of Experimental Physics, University of Wroclaw,
pl. Maxa Borna 9, Wroclaw, 50-204, Poland

pavgaly@gmail.com

The cleavage surface of Sb_2Te_3 layered chalcogenide crystal like as other 2D layered ones, such as InSe, In_4Se_3, InTe, is provided as a nanoscale embossed template for the formation of arrays of self-assembled In nanostructures due to thermal deposition and subsequent solid state dewetting (SSD) procedure. Sb_2Te_3 samples were characterised by *X*–ray diffraction (XRD), *X*–ray photoelectron spectroscopy (XPS), low energy electron diffraction (LEED) and scanning tunneling microscopy/spectroscopy (STM/STS). Sb_2Te_3 has got the anisotropic crystal structure with the presence of van der Waals interlayer interactions. The studied (0001) surfaces were stable with a specific surface relief, which, as in the cases of other layered crystals In_4Se_3, InSe, InTe, is due to the crystal structure of the layer package. The shape of single In induced nanostructure and their array's symmetry are directed by the (0001) surface lattice symmetry. We observed the formation of triangular shaped In nanostructures ordered in hexagonal structured arrays with the well-defined lattice parameter after the SSD. That is, it can be argued that the cleavage (0001) surface of the Sb_2Te_3 crystal actually works as a spatially distributed ordered set of cells, which act as a guiding factor for the self-organization of nanostructures due to SSD process on the macroscale. The comparative fractal analysis of STM images of the (0001) Sb_2Te_3 and (0001) InSe surfaces, shows that distribution in size of In nanostructures are almost the same under commensurate experimental conditions. Sb_2Te_3 energy gap determined from STS spectra of initial surfaces is approaching value of 0.2 eV. An increase in the degree of In coverage is expressed in DOS distribution with appearance of its sufficient value in the range of Sb_2Te_3 energy gap.

Keywords: layered crystal chalcogenides, self-assembled nanostructures, nanostructures' template directed assembly, hetero nanostructures, solid state dewetting, LEED, STM/STS, XPS.

1. Introduction

2D layered chalcogenide semiconductors, such as, InSe, In_4Se_3, InTe, Sb_2Te_3 are among newly emerging materials suitable for functional nanoscale devices applications [1]. It looks like that surface of 2D laye-red crystals are one among most perspective templates for self-assembling of metal nanostructures due to the solid state dewetting [2,3]. Because of intrinsic nature of van der Waals interlayer bonding, layered chalcogenide crystals' surfaces possess

_____

good ambient stability, might be just easily obtained by cleavage even in UHV, and, thus, applied as template for fabrication of metal-semiconductor hetero nanosystems.

Antimony telluride Sb_2Te_3 is one among currently used semiconductor materials for thermoelectric converters to operate within range of room temperatures with high value of thermoelectric efficiency parameter *ZT*. Sb_2Te_3 like as bismuth telluride are often used as components of thermoelectric alloys with thermo-electromotive force 150–220 μV/K. Beside, antimony telluride exhibits nonlinear optical properties [4-6]. All these applications have one basis, namely that antimony telluride Sb_2Te_3 belongs to the class of layered strongly anisotropic semiconductors. The crystalline material contains covalently bonded atoms, forming 5 atoms' thick layers (stacked in order: Te-Sb-Te-Sb-Te), which are bonded to each other by the van der Waals bonds [7]. Due to its layered structure and weak interlayer bond strength, part of Sb_2Te_3 can be mechanically cleaved, exfoliated by adhesive tape or, e.g., by electrochemical procedure [8], to form even a few single layer flakes.

Like other antimony and bismuth chalcogenides, Sb_2Te_3 has got semiconductor properties. Sb_2Te_3 is a narrow-band semiconductor with a band gap of 0.21 eV [9]. It can be converted into both *n*- and *p*-type semiconductors by doping with a suitable impurity. It is also, like Bi_2Se_3, a topological insulator and, therefore, exhibits thickness-dependent physical properties [10].

It is characterized by the presence of a large number of intrinsic defects of the acceptor type, presumably antistructural, i.e., part of the excess antimony atoms takes the place of tellurium atoms – (Sb_{Te}). In such case the high concentration of holes ($p \sim 10^{20}$ cm^{-3}) might be observed, which can be changed only in a narrow range, that complicates the study of the Sb_2Te_3 energy spectrum.

Based on our previous studies of the layered chalcogenides' surfaces [11-13], another potential application of antimony telluride can be expected. The surfaces of layered chalcogenide crystals combine the properties of stable ordered templates along with the weak interaction in the template-deposited layer, which contributes to the formation of ordered metal-semiconductor nanoheterosystems as a result of solid-state dewetting technique (SSD).

In this paper, we focus on the application of (0001) cleavage surface of Sb_2Te_3 layered chalcogenide crystal, as ordered template, suitable for the formation of metal nanostructures' arrays using the SSD. Actually SSD method applications were involved in making arrays of nanoscale particles for electronic and photonic devices and for catalyzing growth of nanotubes and nanowires long enough [14]. One of the key issues in this technology is getting the perfect quality patterned templates and their stability as a basis for output self-organizing structures. However, in contrast to the case of patterned surfaces of layered crystals obtained by cleavage, to achieve this goal in SSD very often it is necessary to apply fairly complex of time-consuming and expensive two-dimensional (2D) fabrication procedures. Among the, so-called, methods of substrate's prepatterning to obtain arrays of nanostructures on it, application of various techniques, such as controlled chemicals, such as selective etching of the substrate surface, galvanic substitution reactions, by which it can be transformed into a template decorated with numerous ordered structures has been reported. Another group of methods includes techniques to form patterns on the surface using lithographic methods, mechanical scribbing, indentation or the use of nanoscale catalysts, which are pre-deposited on the substrate surface, thus forming a certain structure on the surface, the so-called, wetting layer [15-17].

2. Experimental

The Sb_2Te_3 crystal was grown by the Bridgman-Stockbarger method. It should be noted that (0001) Sb_2Te_3 cleavages for XPS and LEED studies were obtained *ex situ* in consequence of experimental constraints. At the same time samples for STM/STS studies were cleaved directly in an UHV. In both cases, the work pieces for cleavage had a special shape of a pedestal and roughly $3x4x6$ mm^3 size. Such shape in combination with Sb_2Te_3 intrinsic bulk anisotropy allow to get several perfect (0001) Sb_2Te_3 cleavage surfaces in consequence of multiple chipping manipulations even *in situ*.

Thermal evaporator EFM-3 was applied for indium deposition in situ. Indium ion current inside the effusion cell was maintained to be constant during the indium deposition. The deposition rate was kept at approximately 0.07 ML/min. Small deposition rates facilitated in producing hetero growth, rather than obtaining of polycrystalline films at high deposition rates. Such rates allowed organizing an activation-migration movement of deposited indium with localization on growth activation centers under consequent annealing at 440–450 K, 3-5 min.

Structural studies were performed using XRD a powder *X*-ray diffractometer "Stoe STADI I" (Germany) with CuKα - wavelength λ=1.540598 Å.

The element-phase composition studies of the surfaces of layered Sb_2Te_3 crystals were performed by XPS method. XPS spectra were acquired by SPECS (PHOIBOS HSA3500 100 R6 [HWType 30:14] MCD 5 (Germany)). An *X*-ray source with the Mg anode MgKα ($E = 1253.6$ eV) was applied. The XPS spectra were recorded in an ultrahigh vacuum of 10^{-10} Torr. The analysis of XPS spectra was performed by SpecsLab Prodigy software.

Low energy electron data (LEED) were acquired by ErLEED 100 optics designed by SPECS Surface Nano Analysis GmbH. The LEED data were analyzed using the SPECS SAFIRE Diffraction Image Acquisition and Processing System for LEED and RHEED.

STM/STS data were obtained by Omicron Nano Technology STM/AFM System operating with UHV better than 10^{-10} Torr at room temperature. The acquisition of STM data was conducted in the constant current mode with spatial resolution 400x400 points regardless of scanned area. STS data were acquired with spatial resolution 80x80 points in current imaging tunnelling spectroscopy (CITS) mode. Free software WS&M v.4.0 from Nanotec Electronica [18] was used while analyzing and processing of STM data.

3. Results and discussion

3.1. Elemental and structural studies of Sb_2Te_3 (0001) surface as template for indium deposition

Fig. 1a shows XPS survey spectrum of the (0001) Sb_2Te_3 surface. XPS spectrum in addition to the main reference maxima of the components of Sb_2Te_3 (Sb 3d$_{5/2}$, Te 3d$_{5/2}$), contains also a substantial maximum of carbon (C 1s). The latter one appears in a consequence of the adsorption from laboratory atmosphere after cleavage. The most intense XPS maxima Sb 3d$_{5/2}$, Te 3d$_{5/2}$, like all others, were identified using a database [19], and recorded in a precise scale of binding energies in order to evaluate new chemical interactions with the transfer of electronic charge on the (0001) surface of the layered Sb_2Te_3 crystal and in its interface layers. Control of the possible charging of the cleavage surface during X-irradiation and XPS spectra recording was necessary because it affects the XPS results (obtained binding energies of chemical elements), thus, the binding energies of the elements were adjusted relatively to the C 1s maximum of carbon (284.5 eV). The results of quantitative analysis, by the method of pure standards, using XPS spectra allow us to conclude about the stoichiometry of the Sb_2Te_3

compound beside the presence of a significant amount of adsorbed carbon. Detailed analysis of extended XPS spectra for Te in the range of binding energies 560–610 eV, which contains the reference maximum Te $3d_{5/2}$ at a binding energy of 572.3 eV and its doublet Te $3d_{3/2}$ and Sb with components Sb $3d_{5/2}$ and Sb $3d_{3/2}$ in the binding energy range of 510-560 eV, also revealed the appearance of peaks of tellurium and antimony oxide phases. However, the concentration of oxygen is much lower than that of carbon. The results of XPS analysis of the initial (0001) surfaces of antimony telluride actually also confirm the data of our previous studies that the surfaces of layered chalcogenide semiconductors obtained *ex situ* tend to be predominantly carbon contaminated [20].

The structural studies of bulk Sb_2Te_3 layered crystals by the of X-ray diffraction (XRD) method and their (0001) cleavage surfaces by the LEED method were conducted.

In consequence of XRD study (see Fig. 1b) the symmetry of the Sb_2Te_3 crystal lattice and its lattice parameters were determined. XRD study shows on rhombohedral crystal structure (R3m space group, lattice parameters **a**=4.2654(8) Å, **c**=30.435(2) Å).
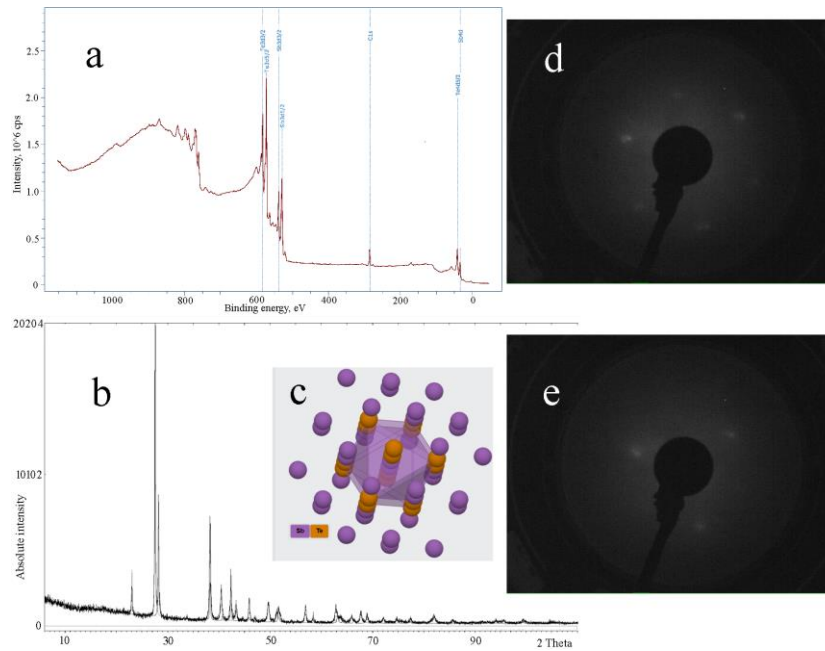
Fig.1. Sb_2Te_3 crystal bulk characterization by: a) XPS survey spectrum, recorded with a resolution of 1 eV and without background correction of the peaks' intensity of chemical elements; b) XRD study (STOE STADI P, CuKα1); c) panoramic model representation of the calculated structural data of the crystal (view towards the surface of the packet - layer) [21] and d, e) Sb_2Te_3 (0001) surface characterization on macroscale by LEED patterns of the as-cleaved sample acquired at a primary electron energies of 78 eV and 112.5 eV.

Fig. 1c represents model of Sb_2Te_3 surface layer calculated using the Vienna Ab initio Simulation Package obtained from the Materials Project [21] a sizable materials database that contains computed structural, electronic, and energetic data for over 33000 compounds. This

model is experimentally confirmed on Fig. 1d that shows LEED pattern of the as-cleaved Sb_2Te_3 sample, acquired at a primary electron energy of 78 eV. Since the diameter of the primary electron beam spot on the crystal surface is about 1 mm, we can conclude that studied templates have got excellent surface structural quality in macroscale according to LEED. LEED shows that the symmetry of the reciprocal lattice of (0001) Sb_2Te_3 doesn't depend on the exposure time at 295 K after cleavage in UHV, and indicates that two-dimensional (2D) lattice on (0001) Sb_2Te_3 cleavages exhibits no reconstruction and is structurally stable at room temperature range and after cleavage *ex situ* at least.

In addition, detailed studies of the intensity dependence of diffraction spots on the primary electrons' energy, as in the case of a layered InSe crystal [22] allow us to conclude that there exhibits a "triangle-like" relief of the Sb_2Te_3 (0001) surface due to vertical displacements of surface layer atoms arranged in sub layers. Fig. 1e shows for example the characteristic LEED spectrum of the (0001) surface at a given energy of primary electron beam, that indicates on the presence of triangular shaped cells, which then could act as a natural relief in the process of self-organized nanostructures forming by the SSD method.

Fig. 2 shows the results of STM study of initial 51.2x51.2 nm^2 Sb_2Te_3 (0001) surface obtained by cleavage *in situ*. Inset on Fig. 2a shows schematically a setup for obtaining multiple quality cleavage surfaces in UHV. The acquired images are essentially noisy as it's shown on Fig. 2a, so, we applied 2D Fast Fourier filtering (see Fig. 2b) to reveal clear surface pattern with ~4.5 Å hexagonal lattice parameter size that is very close to Sb_2Te_3 crystal one in (0001) plane according to XRD data. Zoomed fragment of periodical structure from Fig. 2b is shown on Fig. 2c overlaid by model representation of the corresponding surface lattice.
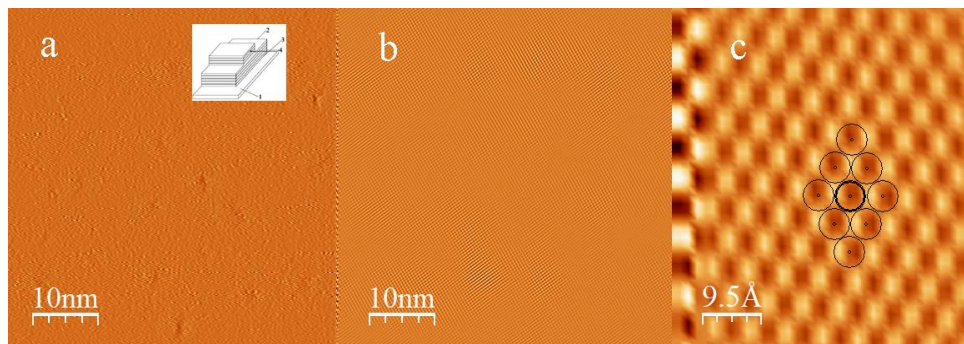
Fig.2. STM study of initial Sb_2Te_3 (0001) substrate: a) STM image 51.2x51.2 nm^2 (tunneling current 124 pA, bias +1.6 V), *Inset*: Schematic image of the sample cleavage in situ: 1 – stainless steel holder, 2 – sample in the form of a "pedestal" suitable for multiple cleavages, 3 – glue or double-sided tape for sample fixing, 4 – stainless steel tip. The arrow indicates the direction of splitting; b) corresponding 2D FFT image; c) zoomed fragment of 2D FFT image 4.7x5.2 nm^2 with characteristic lattice size ~4.5 Å.

Moreover, it should be noted that the detected structure is steadily observed regardless of the time that has passed after the cleavage, which makes it possible, given, as well as the results of the LEED study on the sample surfaces obtained even *ex situ*, unambiguously, to retrieve the lack of Sb_2Te_3 (0001) surface lattice reconstruction, and therefore its suitability as a template for SSD applications.

3.2. STM/STS study of (0001) Sb₂Te₃ crystal surface

Initial Sb$_2$Te$_3$ (0001) surface was subjected to In deposition *in situ*. Fig. 3a shows corresponding STM image acquired after 105 s indium deposition. One could observe rather inhomogeneous surface without visible signs of ordering in the In deposited layer. Next the SSD process was activated. For this purpose the samples with deposited indium were annealed at a temperature of about 170ºC, which is higher than the melting point of indium. Due to the presence of inhomogeneous in height on the nanoscale triangular shaped ordered morphology of Sb$_2$Te$_3$ (0001) surface we could observe formation of similar shaped nanostructures after the SSD, what is also characteristic in the case of the In/InSe (0001) layered chalcogenide crystals' surfaces previously reported [3]. Fig. 3b shows 0D triangular shaped indium self-organized nanostructures induced on (0001) surface Sb$_2$Te$_3$ due to SSD process.
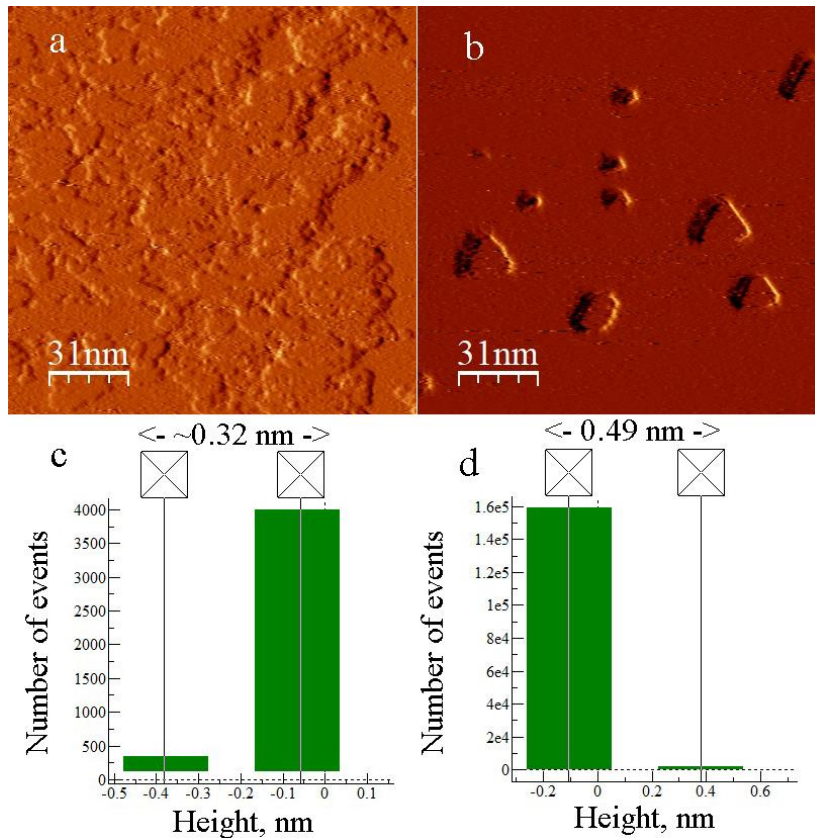
Fig.3. STM study of Sb$_2$Te$_3$ (0001) surface: a) after 105 s indium deposition on substrate (155x155 nm^2 image, tunneling current 101 pA, bias -1.0 V) with subsequent data (c) on height intervals of image pixels; b) after SSD process due to annealing (~170°C) (155x155 nm^2 image, tunneling current 124 pA, bias voltage +1.0 V) with subsequent data (d) on height intervals of image pixels

In addition to the formation of self-assembled indium triangular nanostructures from the obtained STM data one can derive conclusion about the *z* height component of images' pixels.

In the case of Figs. 3a and b the whole array of pixel heights of the corresponding image might be divided into two characteristic subsets (see Figs. 3c and 3d, respectively), what allows us to determine the difference between the average pixel heights of these subsets. For the case of the deposited indium layer on the initial (0001) surface (Fig. 3c), this difference is ~3.2 Å, which, given the 1.56 Å value of the indium atomic radius, confirms the presence of a monolayer of deposited indium. Moreover, the evaluated degree of indium coverage θ of the surface (0001) Sb_2Te_3 is more than 0.9. Thus, looking at the Fig. 3c, we can consider that "basic" observed plane is the surface formed by the deposition of a indium monolayer.

The data on Fig. 3d show that in the result of SSD process the degree of coverage of the initial surface by In decreases significantly, apparently due to the formation of a triangular shaped nano structures, with their height averaging about 1.5 In monolayer (ML), and, in fact, it could reach up to 2 In MLs.

Therefore, all these confirms the viewpoint that the surfaces of layered chalcogenide crystals due to their stability, poor adhesion and relief at the nanoscale can serve as ideal templates for obtaining metal nanostructures with the shapes that are defined by the symmetry of the corresponding surface crystal lattice.

Interesting from the point of view of the formation kinetics of the In/ (0001) Sb_2Te_3 system are the results of the analysis obtained using the Roughness analysis tool in WSxM application shown on Fig. 4a. Curves 1-4 show height distribution acquired in each of points of STM analysis, i.e., pixels on STM images, over 400x400 nm^2 surface areas for initial, indium deposited and consequently annealed samples, respectively. Statistics on the distribution of pixel heights shown by curves 1-4 on Fig. 4a along with the corresponding cases of numerical parameters that characterize the degree of asymmetry of the surface (skewness) and its peakness (kurtosis) presented on inset allow us to draw conclusions how the morphology of the studied surfaces changes. The initial (0001) surface of Sb_2Te_3 (case 1) is sufficiently asymmetric with high degree of peakness. Substantial degrees of indium deposition (case 3) increase the symmetry of the surface layer (skewness parameter equal to zero shows on symmetry of surface's pixels distribution, value above it shows on peaks and below on holes) and lead to an almost Gaussian distribution of heights (kurtosis parameter (peakness) equal to 3.0 is characteristic for Gaussian distribution [23]).

At the same time, further surface heating (case 4) with the activation of SSD processes tends to "restore" asymmetry and peakness. However, in this case we are dealing with the formation of self-organized ordered indium nanostructures on the relief of the antimony telluride (0001) surface pattern.

3.3. STS study of Sb_2Te_3 crystal surface

The changes in Sb_2Te_3 (0001) morphology due to indium deposition when considering heterogeneous metal – semiconductor system are also confirmed by STS data. Fig. 4b shows normalized derivative $(dI/dV)/(I/V)$ curves via bias voltage between probe and studied surface averaged over 150x150 nm^2 area for initial template (curve 1), after In deposition (curve 2) and after the subsequent SSD process (curve 3).

In these cases the densities of the surface states (DOS) that participate in tunneling processes via tip–surface bias voltage are presented. Consequently, Sb_2Te_3 energy gap determined from STS spectra of initial surfaces is approaching value of 0.2 eV. It should be noted that this is not a local value acquired from a single point which contributes to the tunnel current with a diameter of about 1 Å, but appears as a result of averaging the 6400 points STS data of from a sufficiently large area, so, it is consistent with known data obtained by other

methods [6]. Fig. 4b (curves 2, 3) confirms an increase in the degree of indium coverage that is shown by changes in DOS distribution with appearance of its sufficient value in the range of semiconductor Sb_2Te_3 energy gap. However, it should be noted that due to the SSD process (curve 3), the shape of DOS which can be correlated with the valence band (range of negative biases' voltages) and the conduction band (range of positive biases' voltages) of the Sb_2Te_3 crystal tends to be restored relatively to just indium deposited initial template (curve 2).

Surface parameters	initial template (1)	45s In deposition (2)	105s In deposition (3)	annealed (4)
Skewness	1.0613	1.1475	0.0165	0.7762
Kurtosis	32.6093	10.3125	3.2588	9.6445
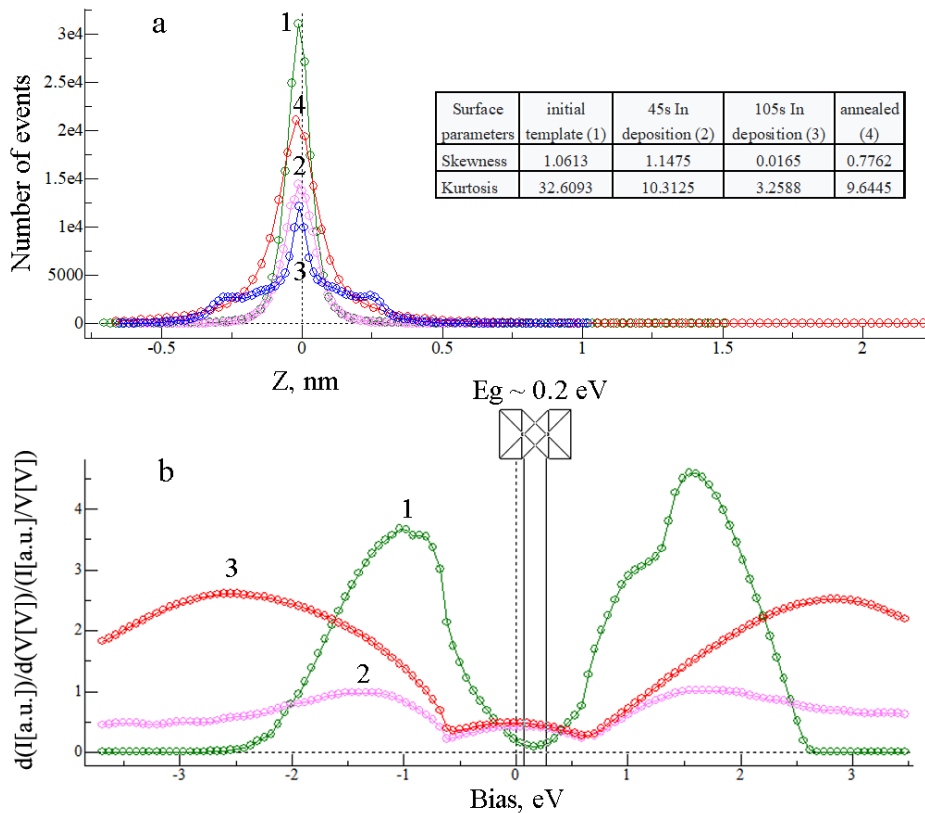
Fig.4. STM/STS study of Sb_2Te_3 (0001) surface: a) height distribution of pixels for 400x400 nm^2 STM images on (0001) Sb_2Te_3 surface before and after indium deposition: 1 – initial, 2 – 45 s deposition, 3 – 105 s deposition, 4 – annealed (~170°C). *Inset table* presents corresponding values of surface parameters ; b) averaged STS data over 6400 curves acquired from 150x150 nm^2 areas indicating initial surface's band gap ~0.2 eV (1, green curve) and energy spectra indicating sufficient value of DOS within band gap after 105 s indium deposition (2, violet curve) and after SSD process due to annealing (~170°C) (3, red curve).

3.4. STM study of indium nanostructures arrangement on (0001) Sb_2Te_3 crystal surface

The study of the formation of indium nanostructures, in fact on a macro scale, on the (0001) Sb_2Te_3 crystal surface is shown on Fig. 5. For this study, we used the results of STM

analysis of surface areas measuring 1x1 μm². Fig. 5a shows as acquired STM image with indium nanostructures spatially distributed in some order. Given the rather different height and triangular dimensions of these nanostructures, which have already been shown in Fig. 3, it is visually difficult to draw a conclusion about the nature of their ordering. However, the application of 2D Fast Fourier Transform (FFT) filtering to selected raw STM images, a fragment of which is shown in Fig. 5b, shows, as expected, hexagonal structure with the well-defined lattice parameter. That is, it can be argued that the cleavage (0001) surface of the Sb_2Te_3 crystal actually works as a spatially distributed ordered set of cells, which act as a guiding factor for the self-organization of nanostructures due to SSD process on the macroscale.

Usually the dimensions of such triangular structures are larger than the actual parameters of the (0001) surface lattice of Sb_2Te_3 while maintaining the shape of the guide pattern. Moreover, the dimensions of these triangles are distributed in magnitude. This phenomenon is referred to as the Gibbs-Thomson effect which works in the nucleation of indium atoms in the SSD process and is based on achieving the, so-called, critical size of the nucleus, above which nanostructure continues to grow, and below it dissolves [23].
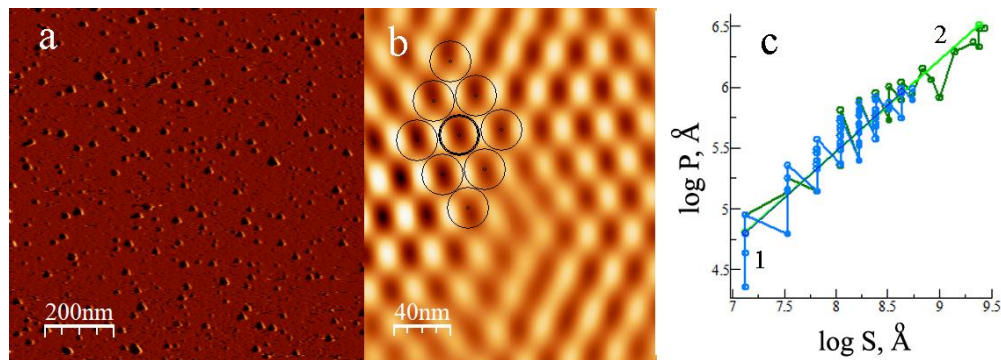
Fig.5. STM study of In/(0001)Sb_2Te_3 2D layered semiconductor nanosystem: a) 1x1 μm² STM image (tunneling current 124 pA, bias +1.0 V) with indium nanostructures after SSD processing; b) zoomed fragment 200x242.5 nm² of 2D FFT image showing on hexagonal like ordering of indium nanostructures with subsequent lattice model well fitted under ~29 nm parameter; c) fractal analysis of triangular shaped indium nanostructures formed on 1x1 μm² areas of: (0001) Sb_2Te_3 (1 – blue circles (experimental data) and (0001) InSe surfaces (2 – green circles (experimental data) and corresponding in colour approximations.

Given the similarity of the symmetry of the (0001) Sb_2Te_3 and (0001) InSe surfaces [18], which is confirmed by the results of the corresponding analyses by LEED and STM methods, we performed a fractal analysis of STM images of these surfaces under comparable experimental conditions in SSD formation of indium nanostructures.

Fig. 5c shows that corresponding approximations of log $P = f(log S)$ dependencies for self-similar shapes have the same slope in both cases. From the point of view of fractal analysis, the distribution in size of indium nanostructures are almost the same on these crystal templates under commensurate conditions – the amount of predeposited indium, the temperature and heating time in the process of SSD. That is, the last parameters, due to the

anisotropy of the properties of chalcogenide layered crystals and the lack of strong interactions between the crystal surface and the deposited layer of indium, make it possible to control the probability of nucleation of metal nanostructures or modulate free interfacial energy influencing critical size of indium nucleus.

4. Conclusions

Surface of 2D Sb_2Te_3 layered semiconductor crystal was applied as template for directed assembly of indium nanostructures. The studied surfaces were stable and have a specific surface relief, which, as in the cases of previously studied layered crystals In_4Se_3, InSe, InTe, is due to the crystal structure of the layer package. Thereby, as well as the anisotropic crystal structure with the presence of van der Waals interlayer interactions, (0001) Sb_2Te_3 crystal surface allows the formation of triangular shaped indium nanostructures ordered in arrays in the SSD process, that is, could be used as template. Moreover, it was found that for the process of SSD indium nanostructuring, despite the different chemical composition of the template Sb_2Te_3 or InSe, as a compound, the similarity of the symmetry of the (0001) Sb_2Te_3 and (0001) InSe surfaces' nanosized relief that determines the shape and ordering of deposited nanostructures and the following parameters in SSD process are decisive: the amount of predeposited indium, the heating temperature and annealing time.

REFERENCES

[1] *Vorobeva N.S., Lipatov A., Torres A. et al.* Anisotropic Properties of Qusi-1D In_4Se_3: Mechanical Exfoliati-on, Electronic Transport, and Polarization-Dependent Photoresponse // Advanced Functional Materials. - 2021. - Vol. 31, Is. 52. - P. 2106459.

[2] *Galiy P.V., Nenchuk T.M., Ciszewski A. et al.* InTe surface application as template for indium deposited nanosystem formation // Molecular Crystals and Liquid Crystals. - 2021. - V. 721, No 1. - P. 1-9.

[3] *Galiy P.V., Nenchuk T.M., Mazur P. et al.* Self-assembled indium nanostructures formation on InSe (0001) surface // Applied Nanoscience. - 2020. - Vol. 10, Is. 12. - P. 4629-4635.

[4] *Zybala R., Mars K., Mikula A. et al.* Synthesis and Characterization of Antimony Telluride for Thermoelectric and Optoelectronic Applications // Arch. Metall. Mater. - 2017. - Vol. 62. - P. 1067-1070.

[5] *Witting I.T., Ricci F., Chasapis T.C. et al.* The Thermoelectric Properties of n-Type Bismuth Telluride Research: Bismuth Selenide Alloys $Bi_2Te_{3-x}Se_x$ // Research. - 2020. - Vol. 10. – P. 1-15.

[6] *Lawal A., Shaari A., Ahmed R., Jarkoni N.* Sb_2Te_3 crystal a potential absorber material for broadband photodetector: A first-principles study // Results in Physics. - 2017. - Vol. 7. - P. 2302-2310.

[7] *Anderson T.L., Krause H.B.* Refinement of the Sb_2Te_3 and Sb_2Te_2Se structures and their relationship to nonstoichiometric $Sb_2Te_{3-y}Se_y$ compounds // Acta Cryst. - 1974. - Vol. B30. - P. 1307-1310.

[8] *López Marzo A.M., Gusmão R., Sofer Z., Pumera M.* Towards Antimonene and 2D Antimony Telluride through Electrochemical Exfoliation // Chemistry A European Journal. - 2020. - Vol. 26, No 29. - P. 6583-6590.

[9]   *Madelung O., Rössler U., Schulz M.* Antimony telluride (Sb_2Te_3) band structure, energy gap Landolt-Börnstein - Group III Condensed Matter, Volume 41C (Non-Tetrahedrally Bonded Elements and Binary Compounds I). - Springer-Verlag: Berlin Heidelberg, 1998.

[10] *Bhunia H., Bar A., Bera A., Pal A.J.* Simultaneous observation of surface- and edge-states of a 2D topological insulator through scanning tunneling spectroscopy and differential conductance imaging // Phys. Chem. Chem. Phys. - 2017. - Vol. 19. - P. 9872-9878.

[11] *Galiy P.V., Mazur P., Ciszewski A., Nenchuk T.M., Yarovets' I.R.* Scanning tunneling microscopy/spectroscopy study of In/In_4Se_3 (100) nanosystems. // The European Physical Journal Plus. – 2019. -Vol. 134, Is. 2. - P. 70-75.

[12] *Galiy P.V., Musyanovych A.V., Buzhuk Ya.M.* The Interface Microscopy and Spectroscopy on the Cleavage Surfaces of the In_4Se_3 Pure and Copper Intercalated Layered Crystals. // Physica E: Low-dimensional Systems and Nanostructures. – 2006. -Vol. 135, Is. 1. - P. 88-92.

[13] *Dhingra A., Marzouk Z.G., Mishra E. et al.* Indium segregation to the selvedge of In_4Se_3 (001). // Physica B: Condensed Matter. – 2020. -Vol. 593. - P. 412280-412282.

[14] *Thompson C.V.* Solid-State Dewetting of Thin Films // Annual Review of Materials Research. - 2012. - Vol. 42. - P. 399-434.

[15] *Oliva-Ramírez M., Wang D., Flock D. et al.* Solid-State Dewetting of Gold on Stochastically Periodic SiO2 Nanocolumns Prepared by Oblique Angle Deposition // ACS Appl. Mater. Interfaces. - 2021. - Vol. 13, No 9. - P. 11385-11395.

[16] *Kumar P.* Trench-template fabrication of indium and silicon nanowires prepared by thermal evaporation process // Journal of Nanoparticle Research. - 2010. - Vol. 12. - P. 2473-2480.

[17] *Lah N.A.C., Trigueros S.* Synthesis and modelling of the mechanical properties of Ag, Au and Cu nanowires // Science and Technology of Advanced Materials. - 2019. - Vol. 20, No 1. – P. 225-261.

[18] *Horcas I., Fernandez R., Gomez-Rodríguez J.M. et al.* WSXM: A software for scanning probe microscopy and a tool fornanotechnology // Rev.Sci.Instrum. - 2007. - Vol. 78. - P. 013705.

[19] Department of Commerce, NIST X-ray Photoelectron Spectroscopy Database, NIST Standard Reference Database Number 20. - National Institute of Standards and Technology, Gaithersburg MD, 2000.

[20] *Galiy P.V., Nenchuk T.M., Stakhira J.M., Fiyala Ya.M.* Auger electron spectroscopy studies of In_4Se_3 layered crystals. // Journal of electron spectroscopy and related phenomena. - 1999. - Vol. 105, No 1. - P. 91-97.

[21] *Jain S.P., Ong G., Hautier W. et al.* Commentary: The Materials Project: A materials genome approach to accelerating materials innovation // APL Materials. - 2013. - Vol. 1, Is. 1. - P. 011002.

[22] *Wang J., Zhu D.* Interfacial Mechanics: Theories and Methods for Contact and Lubrication. - Boca Raton, FL: CRC Press/Taylor & Francis Group, 2019.

[23] *De Yoreo J.J., Vekilov P.G.* Principles of Crystal Nucleation and Growth // Reviews in Mineralogy and Geochemistry. - 2003. - Vol. 54, No 1. - P. 57-93.

64   P.V. Galiy, T.M. Nenchuk, A. Ciszewski, et al.

ISSN 2224-087X. Electronics and information technologies. 2022. Issue 17

ФОРМУВАННЯ САМООРГАНІЗОВАНОЇ НАНОСИСТЕМИ МЕТАЛІЧНИЙ In / ПОВЕРХНЯ (0001) Sb₂Te₃ 2D ШАРУВАТОГО НАПІВПРОВІДНИКА ЯК НАПРАВЛЯЮЧИЙ ШАБЛОН

П.В. Галій[1], Т.М. Ненчук[1], А. Ціжевський[2], П. Мазур[2], О.В. Цветкова[1], В.І. Дзюба[1], Т.Р. Макар[1]

[1]Львівський національний університет імені Івана Франка,
вул. Драгоманова, 50, 79005 Львів, Україна

[2]Institute of Experimental Physics, University of Wroclaw,
pl. Maxa Borna 9, Wroclaw, 50-204, Poland

pavgaly@gmail.com

Наведені результати експериментальних досліджень поверхонь сколювання шаруватого халькогенідного кристалу Sb₂Te₃. Встановлено, що 2D поверхні сколювання (0001) Sb₂Te₃ є придатні для використання у якості нанорозмірного рельєфного шаблону для формування масивів індієвих самоорганізованих наноструктур та наносистем In/(0001) Sb₂Te₃ при його термічному осадженні *in situ* та процедури вторинного твердотільного змочування (ВТЗ). Зразки шаруватих напівпровідників Sb₂Te₃, їх поверхні сколювання (0001) Sb₂Te₃ та наносистеми In/(0001) Sb₂Te₃ на їх основі характеризували і досліджували методами: Х-променевої дифракції; кристалографію поверхонь (0001) Sb₂Te₃ – дифракцією повільних електронів (ДПЕ); фазово-елементний склад – Х-фотоелектронною спектроскопією (ХФЕС) а топографію поверхонь і наносистем – скануючою тунельною мікроскопією/спектроскопією (СТМ/СТС). Встановлено, що поверхні (0001) Sb₂Te₃ є стабільними з особливим рельєфом, що, як і у випадках інших шаруватих кристалів, зумовлено кристалічною структурою шар-пакету. Форма окремої індієвої наноструктур In/(0001) Sb₂Te₃ та симетрія їх масивів (наносистем) визначаються симетрією поверхневої ґратки (0001). Встановлено формування In наноструктур трикутної форми, упорядкованих у гексагональні структуровані масиви з виразним параметром поверхневої ґратки після ВТЗ. Поверхня сколювання (0001) Sb₂Te₃ працює як просторово розподілений впорядкований набір комірок, і є направляючим фактором для самоорганізації наноструктур завдяки ВТЗ у макромасштабі. Порівняльний фрактальний аналіз СТМ-зображень поверхонь (0001) Sb₂Te₃ і (0001) InSe із сформованими масивами наноструктур показує, що розподіл за розмірами наноструктур індію майже однаковий у співмірних експериментальних умовах. Величина забороненої зони Sb₂Te₃, визначена за спектрами СТС вихідних поверхонь, є близькою до 0,2 eB. Збільшення ступеня покриття поверхні In зумовлює зміну розподілу густини енергетичних станів наносистем In/(0001) Sb₂Te₃ з появою її суттєвої величини в діапазоні забороненої зони Sb₂Te₃.

Ключові слова: шаруваті халькогенідні кристали, самоорганізовані наноструктури, збірка наноструктур керована шаблоном, гетеронаноструктури, вторинне твердотільне змочування, комплекс методик – ДПЕ, СТМ/СТС, ХФЕС, Х-променева дифракція.